Polymer Journal (2013) 45, 173–178

www.nature.com/pj

ORIGINAL ARTICLE

Coagulation dimension of freezable bound solvent in isotactic polypropylene/*o*-dichlorobenzene gel

Narumi Fujiwara[1], Hiroyuki Tanimura[1], Tsunehiko Nakasugi[1], Takahiko Nakaoki[1], Kazuko Inoue[1], Junpei Miki[1], Manshi Ohyanagi[1], Daisuke Yamaguchi[2] and Satoshi Koizumi[2]

The coagulation size of a solvent bound in an isotactic polypropylene (iPP)/*o*-dichlorobenzene gel was estimated by thermal analysis and small-angle neutron scattering (SANS), and it was examined with respect to the molecular morphology of the gel. The melting process of the solvent frozen in the iPP/*o*-dichlorobenzene gel showed an endothermic peak below the melting temperature of pure *o*-dichlorobenzene. This temperature decrease is closely related to the coagulation size of the freezable bound solvent. The relationship between the decrease in the melting temperature and the coagulation size of *o*-dichlorobenzene was estimated by using porous silica gel. Then, an equation was applied to estimate the coagulation size of the solvent in the iPP gel. The 20-wt% gel showed a coagulation radius of 6.1 nm, whereas for the 50-wt% gel, the radius decreased to 4.1 nm. Next, a SANS measurement was taken for comparison purposes (to be compared with the coagulation size determined by the thermal analysis). The coagulation dimension was estimated using the scattering profile of iPP/*o*-dichlorobenzene-d_4. The coagulation radius of the freezable bound solvent decreased from 4.8 nm for the 20-wt% gel to 4.0 nm for the 50-wt% gel. This result showed good agreement with the estimations from the thermal analysis.
Polymer Journal (2013) **45,** 173–178; doi:10.1038/pj.2012.126; published online 27 June 2012

Keywords: bound solvent; gel; isotactic polypropylene; SANS; thermal analysis

INTRODUCTION

Isotactic polypropylene (iPP) is a representative crystalline polymer. Many studies have been conducted on the molecular structure of iPP. The iPP chain can organize into various spatial arrangements, giving rise to three different crystalline polymorphs: α-monoclinic, β-hexagonal and γ-orthorhombic forms.[1–8] In these crystalline forms, the α-form is known as the most stable crystalline form. The gelation of a crystalline polymer, such as iPP, is closely associated with the formation of crystalline phases at cross-linking points.[9] The molecular morphology of iPP gel is characterized by spherulites.[10,11] During the early stages of gelation, small crystals, such as fringed micelles, act as cross-linking points, giving rise to the formation of spherulites. A study on the crystalline structure formed in iPP/*o*-dichlorobenzene gel was conducted using solid-state high-resolution carbon-13[1] nuclear magnetic resonance spectroscopy.[12] The stable crystalline α-form provides a doublet with an intensity ratio of 2:1 for methylene resonance; however, the crystalline phase formed in the gel forms a doublet with the opposite intensity ratio. Therefore, the disordered α-form correlates to the gel-forming crystal.

Most studies on such gels have focused on the molecular structure at cross-linking points, but there are few reports on the coagulation of a solvent bound in the gel. Higuchi *et al.*[13] investigated the melting behavior of water in a polyvinyl alcohol (PVA) swollen gel and showed the existence of free and freezable bound water. The coagulation dimension of a solvent is closely related to the decrease in melting temperature. A thermodynamic equation describing this relationship was proposed by Gibbs and Thomson.[14] According to the equation, the coagulation radius is inversely proportional to the decrease in temperature. Recently, Nedelec *et al.*[17] reported that the coagulation radius estimated by differential scanning calorimetry (DSC) measurements can be described by an exponential function.[15–19] The former relationship corresponds to the first-order Taylor polynomial of the latter one. By using the first-order approximate function,[20,21] we reported the coagulation dimension of water in a PVA hydrogel formed from freeze/thaw cycles.[22] The coagulation radius of water was 15.1 nm for a 10-wt% gel, which is comparable to the average diameter of 30 nm reported from transmission electron microscopy measurements.[23] Recently, the melting behavior of a solvent in a non-hydrogel, iPP/*o*-dichlorobenzene, was reported by our group.[10,11] It was confirmed that there are two melting peaks for *o*-dichlorobenzene in the gel. One is a sharp melting peak at the same temperature as that of pure *o*-dichlorobenzene and the other is a very broad peak observed at a lower temperature than that of the pure solvent. The respective

[1]Department of Materials Chemistry, Innovative Materials and Processing Research Center, Ryukoku University, Otsu, Japan and [2]Science Research Center, Japan Atomic Energy Agency, Tokai-mura, Japan
Correspondence: Professor T Nakaoki, Department of Materials Chemistry, Innovative Materials and Processing Research Center, Ryukoku University, Seta, Otsu 520-2194, Japan.
E-mail: nakaoki@rins.ryukoku.ac.jp
Received 27 December 2011; revised 12 April 2012; accepted 10 May 2012; published online 27 June 2012

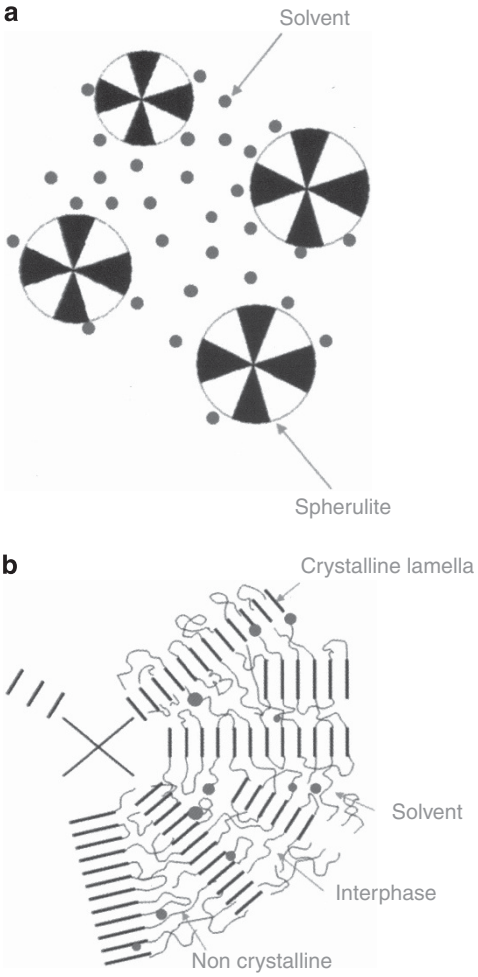

Figure 1 Schematic model of bound solvent in the gel. (**a**) Free solvent in the gel, which provides the same melting temperature as that of the pure solvent, would be located between spherulites. (**b**) Freezable bound solvent with a lower melting temperature than that of the pure solvent would be located in the non-crystalline region between lamellae in spherulites. A full color version of this figure is available at *Polymer Journal* online.

solvents with those melting peaks were assumed to be free and freezable bound solvents. The solvent molecules can be located only in the non-crystalline region (that is, not in the crystalline region). There are two non-crystalline regions in iPP gel: one is a comparatively large region between spherulites that contains the free solvent and the other is a non-crystalline phase between lamellae in the spherulites that contains the freezable bound solvent. A schematic model of this configuration of phases is shown in Figure 1.

The purpose of this study was to determine the coagulation size of the solvent bound in iPP/*o*-dichlorobenzene by thermal analysis. Then, this size was compared with the dimension estimated by small-angle neutron scattering (SANS).

EXPERIMENTAL PROCEDURE

Material

An iPP sample was supplied by Showa Denko Co. Ltd (Tokyo, Japan) and purified by Soxhlet extraction with n-heptane. The average molecular weight (M_w) and meso triad (mm) were estimated to be 3.9×10^5 and 98.5%, respectively. The gel was prepared as follows. Both iPP and *o*-dichlorobenzene were placed in an ampoule, degassed *in vacuo* and sealed. The solution was homogeneously dissolved at 160 °C and then quenched at 0 °C. The gel was kept at 0 °C for 24 h to produce a stable gel. The concentration of iPP increased from 10 to 80 wt%.

Porous silica gels were purchased from Sigma Aldrich (Tokyo, Japan) and Fuji Silysia Chemical Ltd (Tokyo, Japan). The pore radii were 4.5, 7.3 and 8.6 nm for the Sigma Aldrich gels and 22.4 nm for the Fuji Silysia gel.

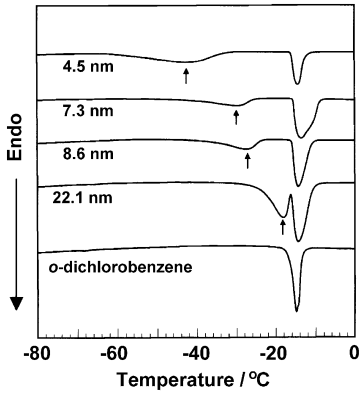

Figure 2 Melting process of *o*-dichlorobenzene filling the porous silica gel. The pore radius is shown on the left side of the figure.

DSC measurement

Thermal analysis was performed using a Rigaku DSC 8230D calorimeter (Rigaku, Tokyo, Japan). Samples were scanned at a heating rate of 5 °C min^{-1} under nitrogen flow. The measurements were taken between −100 °C and room temperature.

SANS measurement

Neutron scattering measurements were conducted at the Japan Atomic Energy Agency SANS-J. The SANS profile was measured using a low-temperature cryostat. A wavelength of 0.65 nm was used. The sample-to-detector distances were 10.2 and 2.25 m. A quartz cell was used as a sample holder, and the scattering intensity was normalized by aluminum. Deuterated *o*-dichlorobenzene and normal iPP were used for the measurements. Incoherent scattering from hydrogenated iPP was eliminated by subtracting the scattering of iPP from that of the gel.

Relationship between decrease in temperature and coagulation dimension of *o*-dichlorobenzene

Ishikiriyama *et al.*[20] reported on the relationship between the radius of ice and the decrease in the melting temperature of ice filling a porous silica gel, which is derived from the Gibbs–Thomson equation. However, there are no reports on the relationship between the coagulation size and the decrease in the melting temperature for *o*-dichlorobenzene. Therefore, the coagulation radius of *o*-dichlorobenzene was estimated as a function of the decrease in temperature from the melting point of the pure solvent (ΔT) by following Ishikiriyama *et al.*'s procedure. The coagulation radius of the freezable solvent $r(T)$ is related to the decrease in temperature as follows:

$$r(T) = \frac{\alpha(T)}{\Delta T} \tag{1}$$

where $\alpha(T)$ is a thermodynamical parameter. For spherical ice, $\alpha(T)$ has been reported to be $33.41–0.0959\Delta T$.[20] Ishikiriyama *et al.*'s procedure was applied to estimate the coagulation radius of freezable *o*-dichlorobenzene. Four silica gels with different pore radii were used to obtain a calibration curve between the pore radius of the silica gel and the decrease in the melting temperature of *o*-dichlorobenzene. Figure 2 illustrates the melting process of *o*-dichlorobenzene filling the silica gels. Two melting peaks due to *o*-dichlorobenzene were observed by DSC measurements. One corresponds to the melting of normal *o*-dichlorobenzene near −17 °C and the other was observed at a lower temperature. The latter corresponds to the melting of the solvent filling the

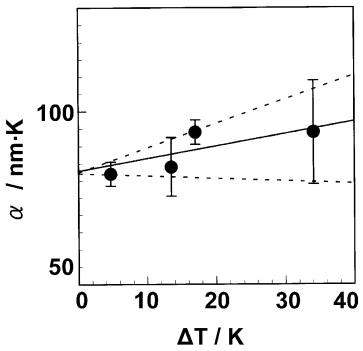

Figure 3 Parameter $\alpha(T)$ in Equation (1) as a function of a decrease in temperature. The solid line is the fit estimated by average values. The maximum and minimum values are indicated by broken lines.

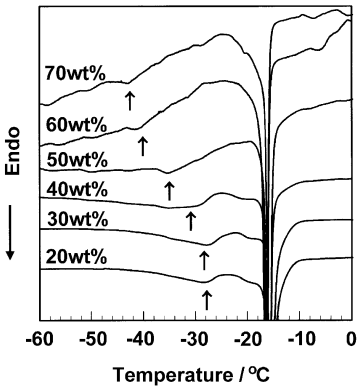

Figure 4 DSC chart of the melting process of *o*-dichlorobenzene in the iPP/*o*-dichlorobenzene gel depending on concentration.

pores, that is, the *o*-dichlorobenzene filling the smaller pores showed a lower melting temperature. Following the analytical procedure of a previous study,[20] $\alpha(T)$ was plotted against the decrease in melting temperature in Figure 3. The experimental result can be described by the following equation:

$$\alpha(T) = 0.356\ \Delta T + 82.9 \qquad (2)$$

This equation was applied to estimate the coagulation radius of *o*-dichlorobenzene in the gel.

RESULTS AND DISCUSSION

Coagulation dimension of solvent in the iPP gel

Figure 4 shows a DSC chart of the melting process of the solvent in the iPP/*o*-dichlorobenzene gel. In addition to the endothermic peak due to normal *o*-dichlorobenzene at $-17\,^{\circ}C$, the low melting peak due to the freezable bound solvent was observed for *o*-dichlorobenzene in the gel. The melting enthalpy of the freezable bound solvent reduced with increasing concentration and then disappeared above 70 wt%. This indicates that all of the solvent adopted a non-freezable state. The melting temperature decreased as the concentration increased. For example, the decrease in temperature for the normal *o*-dichlorobenzene was as large as $15\,^{\circ}C$ for the 20-wt% gel and became even greater for the high-concentration gel. The Gibbs–Thomson equation is derived from the Laplace equation.[24] According to the Laplace equation, the pressure difference between a solid and liquid is equal to the surface energy, which depends on the curvature of coagulation. The curvature of coagulation is an important factor that determines the melting temperature. A small coagulation with large curvature tends to melt at a lower temperature. Equation (1) was applied to estimate the coagulation size of the solvent in the gel. Figure 5 plots the coagulation radius of *o*-dichlorobenzene as a function of concentration in the iPP gel. The coagulation radius decreased with increasing concentration. For example, the coagulation radius of the 20-wt% gel was 6.1 nm, whereas the radius was as small as 4.1 nm for the 50-wt% gel. It has been suggested that the freezable solvent is located in the amorphous region between lamellae in the spherulite.

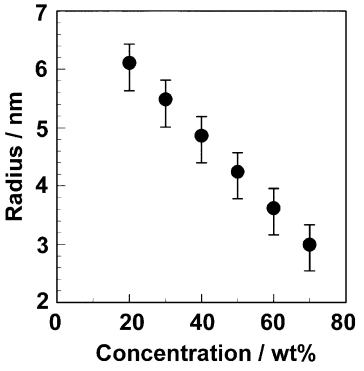

Figure 5 Coagulation radius of *o*-dichlorobenzene in the iPP gel depending on concentration.

SANS measurement of iPP gel depending on temperature

It has been demonstrated that thermal analysis is one of the most powerful tools used to evaluate the coagulation dimension of solvents in a gel. However, it is not a direct method for determining the coagulation dimension. In contrast, the structure of an iPP gel, including the coagulation of the solvent, can be observed in reciprocal space by using the scattering technique; hence, SANS measurements were carried out. The coagulation size of the solvent in the gel that was evaluated by the SANS profile was then compared with the results that were obtained using thermal analysis. Figure 6 shows the SANS profile of the 30-wt% iPP/*o*-dichlorobenzene-d_4 gel observed between -60 and $0\,^{\circ}C$. The scattering profile changed in intensity around $q = 0.1\,nm^{-1}$ between -40 and $-30\,^{\circ}C$. The fact that this temperature range contains the melting point of the freezable bound solvent determined by thermal analysis (as indicated by the arrows in Figure 4) suggests that the SANS profile does reflect the structure of freezable solvents. The total SANS profile shown in Figure 6a seems to possess two types of Guinier regions, which are located at $q \sim 0.007$ and $\sim 0.5\,nm^{-1}$, respectively, and are indicative of a hierarchical structure for the coagulation of the solvent. Thus, we analyzed the SANS profiles by fitting with a calculated scattering function, $I(q)$, containing two types of structural units that were previously reported by Beaucage *et al.*[25]

$$I(q) = G_1 \exp\left(-\frac{q^2 R_{g,1}^2}{3}\right) + B_1 \exp\left(-\frac{q^2 R_{g,2}^2}{3}\right) \times \left\{\left[erf\left(qR_{g,1}/\sqrt{6}\right)\right]^3/q\right\}^{P1} + G_2 \exp\left(-\frac{q^2 R_{g,2}^2}{3}\right) + B_2\left\{\left[erf\left(qR_{g,2}/\sqrt{6}\right)\right]^3/q\right\}^{P2} \qquad (3)$$

In Equation (3), q denotes the magnitude of the scattering vector and $R_{g,i}$, G_i and B_i ($i = 1$ or 2) are the radius of gyration (or particle size),

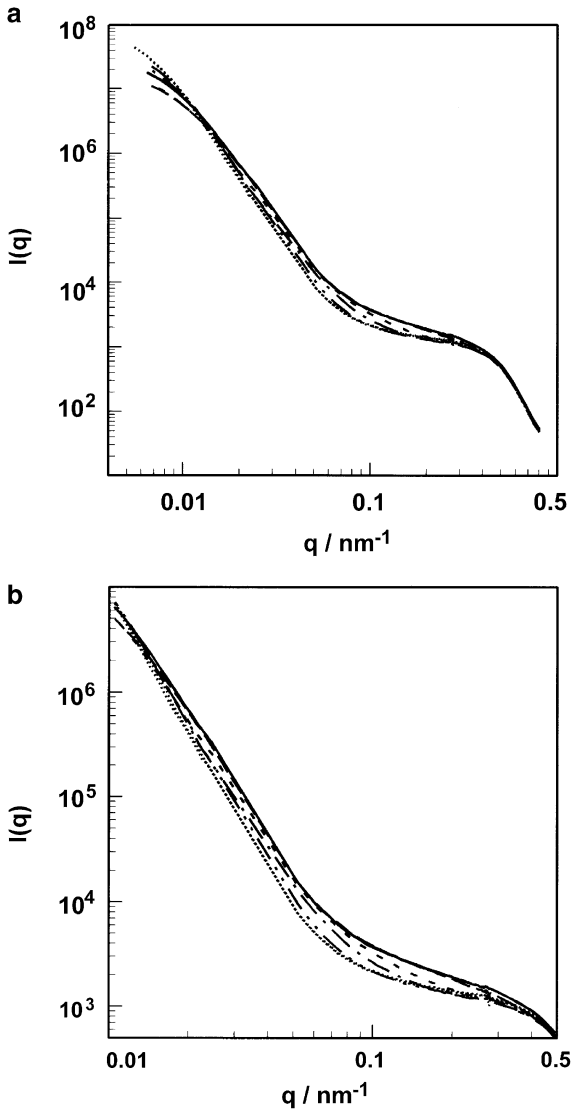

Figure 6 (**a**) Temperature dependence of SANS profile for the 30-wt% iPP/*o*-dichlorobenzene-d_4 gel. (**b**) Expanded profile. The SANS profiles observed at −60 and −50 °C overlapped. These are indicated by a solid line. The profile changed above −40 °C. Then, the profiles at −10 and 0 °C overlapped. These are indicated by a dotted line. ———: −60 °C and −50 °C, – – – –: −40 °C, ------: −30 °C, – · – · – ·: −25 °C, – · · – · · –: −20 °C, ...: −10 °C and 0 °C.

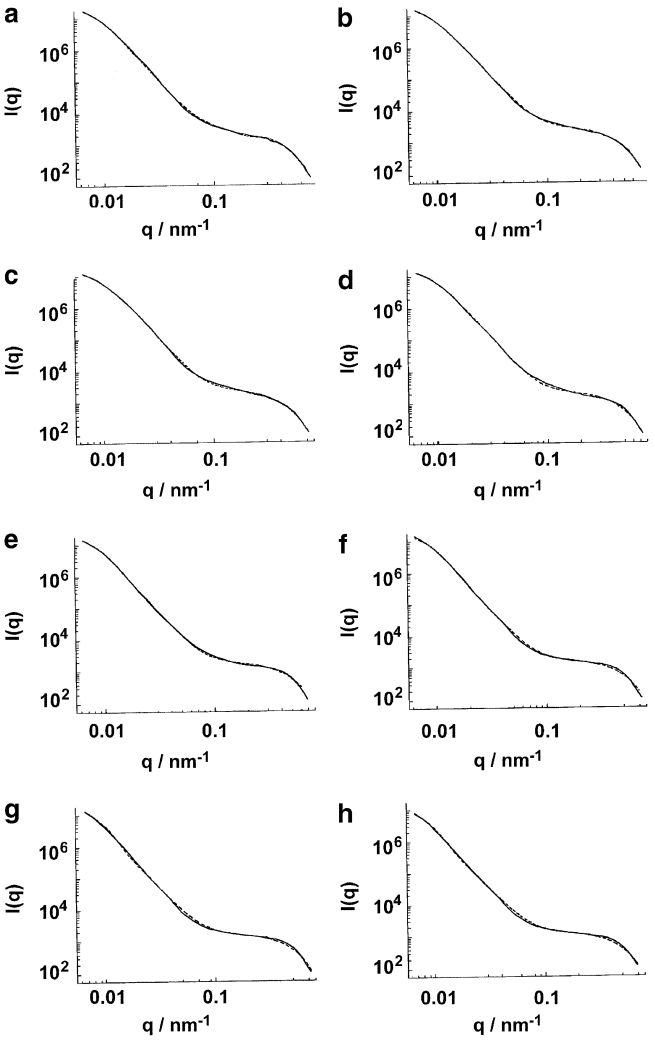

Figure 7 SANS profile of the 30-wt% iPP/*o*-dichlorobenzene-d_4 gel (——) and the theoretical curve (– – –) at: (**a**) −60, (**b**) −50, (**c**) −40, (**d**) −30, (**e**) −25, (**f**) −20, (**g**) −10 and (**h**) 0 °C.

the factor for the low-q scattering of the Guinier region and for the high-q scattering of the low-power region of the i-th level structure, respectively. In the second and fourth terms of Equation (3), $erf()$ is the error function and the power-law index P_i ($i = 1$ or 2) is related to the surface scattering of the i-th level structure. When $P_i = 4$ is satisfied, the Porod law is valid for surface scattering.

Curve-fit analyses were conducted using a trial-and-error method, and the results of the 30-wt% gel are shown in Figure 7. The experimental profile was in good agreement with the calculated profile. Typical values obtained by the curve-fit analyses for the parameters $R_{g,1}$ and $R_{g,2}$ are 35 and 4.5 nm, respectively. For $R_{g,2}$, the obtained value (∼4.5 nm) is comparable to the coagulation size; thus, we can assign the shoulder peak designated by the filled arrow to the scattering from the coagulation of the solvent. However, the value obtained for $R_{g,1}$ (∼350 nm) is not in agreement with the size of the coagulation or that of the spherulite, which was estimated in a previous study as being >30 μm by polarized optical microscopy.[10] For the moment, we will consider that $R_{g,1}$ corresponds to large aggregated coagulations located in the interparticle area of the spherulites. However, the identification of $R_{g,1}$ is beyond the scope of this work, and hereafter we will focus only on the dependence of $R_{g,2}$ on the temperature or on the concentration of iPP. In Figure 8, the coagulation radius of the solvent in the gel is plotted as a function of temperature. The coagulation size was 4.6 nm at −60 °C; this coagulation radius is identical to that observed by DSC. The coagulation size decreased from 4.6 to 4.1 nm between −40 and −30 °C, which corresponds to the melting of the freezable bound solvent. This might be explained by the transfer from the freezable bound to the non-freezable solvents. The coagulated domain of the freezable solvent is surrounded by swollen iPP chains featuring the non-freezable solvent. After the solvent is melted, some of the solvent may penetrate the region of the non-freezable solvent: this will reduce the coagulation size of the freezable solvent.

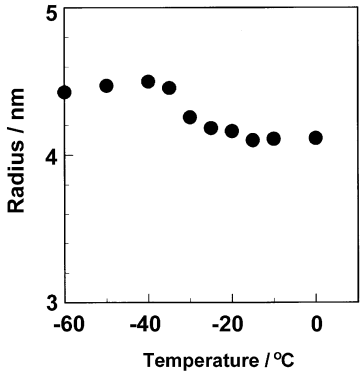

Figure 8 Coagulation radius of freezable bound *o*-dichlorobenzene in the gel as a function of temperature (as estimated by SANS measurement).

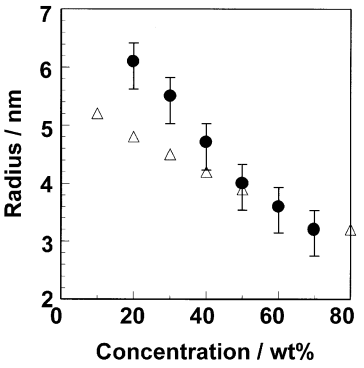

Figure 10 Coagulation radius of freezable bound *o*-dichlorobenzene in the gel. Δ: SANS and ●: DSC.

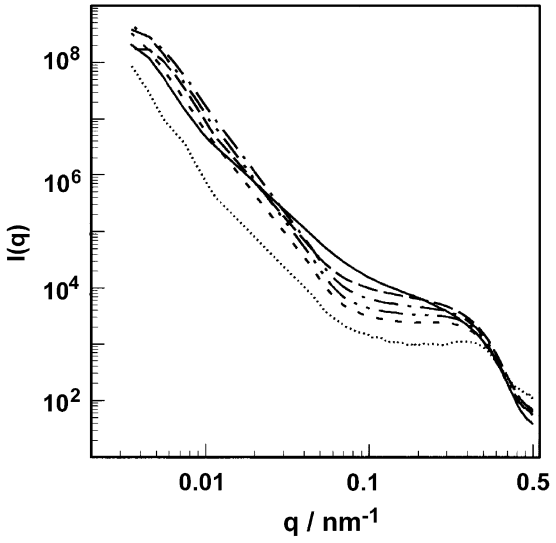

Figure 9 SANS profile for iPP/*o*-dichlorobenzene-d_4 gel depending on concentration. ———: 10 wt% – – –: 20 wt%, – · – · –: 30 wt%, – · · –: 40 wt%, ------: 50 wt%, ...: 80 wt%.

SANS profile of iPP gel depending on concentration

Figure 9 shows the SANS profile of the iPP/*o*-dichlorobenzene-d_4 gel at room temperature as a function of concentration. The scattering profile varied with the concentration. The q-dependence of the scattering intensity profile clearly changed from the 10-wt% gel to the 20-wt% gel, indicating that the size distribution of the solvent coagulation with a low melting temperature changed. Furthermore, from the 20-wt% gel to the 80-wt% gel, the scattering intensity decreased monotonically over the whole observed q-range, suggesting that the number density of the solvent coagulation decreased with the solvent concentration. These trends observed for $I(q)$ with changes in concentration strongly confirm that the obtained SANS profile accurately reflects the structure of the solvent coagulation. The coagulation radius of the freezable bound solvent was estimated by curve-fitting analysis, and Figure 10 shows the dependence of the coagulation radius (represented by the open triangles) on concentration. The coagulation dimension decreased from 4.8 nm for the 20-wt% gel to 4.0 nm for the 50-wt% gel as the concentration increased. The coagulation radius (represented by the closed circles) estimated by thermal analysis is also plotted for reference. Although there is a large distribution in the coagulation size of the solvent, the values are in good agreement. Therefore, it was confirmed that a freezable bound solvent coagulation on the order of a few nanometers exists in the iPP/*o*-dichlorobenzene gel.

In our previous report on a PVA hydrogel, the coagulation size of water in the PVA hydrogel was evaluated as a function of concentration.[22] The coagulation radius for the 10-wt% PVA gel was as large as 15.1 nm but decreased to 1.5 nm for the 70-wt% gel. The coagulation dimension of the PVA hydrogel was on the order of nanometers, comparable to that of the iPP/*o*-dichlorobenzene gel. However, the coagulation size ranged between 1.5 and 15.1 nm and had a very wide distribution in comparison with that of the iPP gel, which ranged from 4.1 nm for the 50-wt% gel to 6.1 nm for the 20-wt% gel. This could be explained by the various molecular morphologies that formed throughout the gelation process. The iPP gel formed a crystal consisting of spherulites, whereas the PVA gel showed low crystallinity because a few crystals did not consist of spherulites.[26–28] In the case of the PVA hydrogel, the phase separation with fluctuations in density may have produced the coagulations of water and the swollen PVA chains containing water in low- and high-density regions, respectively. Therefore, the most important factor determining the coagulation dimension of water is the extent of density fluctuation. Meanwhile, the iPP gel consists of spherulites, which are formed in high-density regions amid density fluctuations. Therefore, a molecular morphology consisting of crystalline and non-crystalline regions would be the most important factor affecting the coagulation size of the solvent. In this study, a quenching temperature of 0 °C was adopted to form a gel. Therefore, the coagulation dimension of *o*-dichlorobenzene bound in the non-crystalline region between crystalline lamellae would vary over a small range depending on concentration.

It has been reported that the freezable bound solvent lies in the non-crystalline region between lamellae in spherulites.[10,11] A structure consisting of repeating lamellar and non-crystalline layers was reported for a bulk iPP crystal by small-angle X-ray scattering analysis.[29] The long-range order of the structure was estimated to be 18.6 nm. Gelation is a type of crystallization in a solution; thus, its long-range order would be on almost the same order as that of the bulk iPP crystal. Because long-range order corresponds to the total thickness of crystalline lamellar and non-crystalline regions, the coagulation dimension of a few nanometers estimated by thermal analysis and SANS can be regarded as a suitable size for coagulations to settle in the non-crystalline region between lamellae. The different molecular morphology of the iPP chain affects the concentration

dependence of the coagulation size of the freezable solvent, that is, the non-crystalline layer will be smaller in a high-concentration gel.

CONCLUSIONS

The coagulation size of freezable bound solvent in an iPP/*o*-dichlorobenzene gel was evaluated using DSC and SANS. In addition to the melting of normal *o*-dichlorobenzene, the melting of freezable bound solvent in the gel was observed; the latter occurred at a lower temperature than the former. The decrease in the melting temperature was interpreted as being affected by the coagulation dimension. A porous silica gel with different pore sizes was used to determine the relationship between the decrease in temperature and the coagulation radius of *o*-dichlorobenzene. This relationship was applied to estimate the coagulation radius of *o*-dichlorobenzene in the iPP gel. The coagulation radius decreased from 6.1 nm for the 20-wt% gel to 4.1 nm for the 50-wt% gel.

Furthermore, SANS measurements were used to estimate the coagulation dimension of the solvent in the gel. The scattering profile of iPP/*o*-dichlorobenzene-d_4 was fitted by a unified scattering function. The coagulation radius of freezable bound solvent was 4.8 nm for the 20-wt% gel and 4.0 nm for the 50-wt% gel; these results were in good agreement with the values estimated by the thermal analysis.

The concentration dependence of the coagulation size was interpreted as a result of the molecular morphology in the spherulite. The freezable bound solvent was located in the non-crystalline region between lamellae. With increasing concentration, the layer length of the non-crystalline region was reduced. This reduced the coagulation dimension of the solvent.

ACKNOWLEDGEMENTS

This work was partially supported by a grant from the High-Tech Research Center Program for private universities by the Japan Ministry of Education, Culture, Sports, Science and Technology.

1 Natta, G., Pino, P., Corradini, P., Danuss, F., Mantica, E., Mazzanii, G. & Moriglio, G. Crystalline high polymer of α-olefins. *J. Am. Chem. Soc.* **77,** 1708–1710 (1955).
2 Natta, G., Corradini, P. & Ganis, P. Prediction of the conformation of the chain in the crystalline state of tactic polymers. *J. Polym. Sci.* **58,** 1191–1199 (1962).
3 Meille, S. V., Ferro, D. R., Bruckner, S., Lovinger, A. J. & Padden, F. J. Structure of β-isotactic polypropylene: a long-standing structural puzzle. *Macromolecules* **27,** 2615–2622 (1994).
4 Sauer, J. A. & Pae, K. D. Structure and thermal behavior of pressure-crystallized polypropylene. *J. Appl. Phys.* **39,** 4959–4968 (1968).
5 Bruckner, S. & Meille, S. V. Non-parallel chains in crystalline γ-isotactic polypropylene. *Nature* **340,** 455–457 (1989).
6 Meille, S. V., Bruckner, S. & Porzio, W. γ-Isotactic polypropylene. A structure with nonparallel chain axes. *Macromolecules* **23,** 4114–4121 (1990).
7 Corradini, P. & Guerra, G. Polymorphism in polymers. *Adv. Polym. Sci.* **100,** 183 (1992).
8 Auriema, F., de Ballesteros, O. R., De Rosa, C. & Corradini, P. Structural disorder in the α form of isotactic polypropylene. *Macromolecules* **33,** 8764–8774 (2000).
9 Nakaoki, T., Shuto, H., Hayashi, H. & Kitamaru, R. High resolution solid-state ^{13}C NMR study of isotactic polypropylene gel. *Polymer* **39,** 3905–3908 (1998).
10 Nakaoki, T. & Harada, S. Melting behavior of bound solvent in isotactic polypropylene/o-dichlorobenzene gel. *Polymer J.* **37,** 429–433 (2005).
11 Nakaoki, T. & Harada, S. Relationship between melting behavior of solvent and molecular morphology for isotactic polypropylene/o-dichlorobenzene gel. *Curr. Trends Polym. Sci.* **10,** 47–54 (2006).
12 Nakaoki, T. & Inaji, Y. Molecular structure of isotactic polypropylene formed from homogeneous solution: gelation and crystallization. *Polymer J.* **34,** 539–543 (2002).
13 Higuchi, A. & Iijima, T. D.s.c. investigation of the states of water in poly(vinyl alcohol) membranes. *Polymer* **26,** 1207 (1985).
14 Gibbs, J. *Collected Works* (Yale University Press, New Haven, CT, 1928).
15 Boyer, S. A. E., Baba, M. & Nedelec, J. -M. Polymer microstructures: modification and characterization by fluid sorption. *Int. J. Thermophys.* **29,** 1907–1920 (2008).
16 Baba, M. & Nedelec, J. -M. Characterization of gels and networks using new calorimetric techniques. *Sol-gel Methods for Materials Processing* 195–211 (2008).
17 Nedelec, J. -M., Grolier, J. P. E. & Baba, M. Thermoporosimetry: A powerful tool to study the cross-linking in gels networks. *J. Sol-gel Sci. Techn.* **40,** 191–200 (2006).
18 Bahloel, N., Baba, M. & Nedelec, J.-M. Universal behavior of linear alkanes in a confined medium: toward a calibrationless use of thermoporometry. *J. Phys. Chem. B* **109,** 1627–1629 (2005).
19 Billamboz, N., Nedelec, J. -M., Grivet, M. & Baba, M. Cross-linking of polyolefins: a study by thermoporosimetry with benzene derivatives as swelling solvents. *Chem. Phys. Chem.* **6,** 1126–1132 (2006).
20 Ishikiriyama, K., Todoki, M. & Motomura, K. Pore size distribution (PSD) measurements of silica gels by means of differential scanning calorimetry: I. optimization for determination of PSD. *J. Colloid Interface Sci.* **171,** 92–102 (1995).
21 Ishikiriyama, K. & Todoki, M. Pore size distribution measurements of silica gels by means of differential scanning calorimetry: II. thermoporosimetry. *J. Colloid Interface Sci.* **171,** 103–111 (1995).
22 Nakaoki, T. & Yamashita, H. Bound states of water in Poly(vinyl alcohol) hydrogel prepared by repeated freezing and melting method. *J. Mol. Struct.* **875,** 282–287 (2008).
23 Willcox, P. J., Howie, D. W., Shimidt-Rohr, K., Hoagland, D. A., Gido, S. P., Pudjijanto, S., Kleiner, L. W. & Venkatraman, S. Microstructure of poly(vinyl alcohol) hydrogels produced by freeze/thaw cycling. *J. Ploym. Sci. Part B Polym. Phys.* **37,** 3438 (1999).
24 Landel, M. R. Thermoporometry by differential scanning calorimetry: experimental considerations and applications. *Thermochimica Acta* **433,** 27–50 (2005).
25 Beaucage, G., Kammler, H. K. & Partsinis, S. E. Particle size distributions from small-angle scattering using global scattering functions. *Appl. Crystallography* **37,** 523–535 (2004).
26 Ricciardi, R., Auriemma, F., De Rosa, C. & Laupretre, F. X-ray diffraction analysis of poly(vinyl alcohol) hydrogels, obtained by freezing and thawing techniques. *Macromolecules* **37,** 1921–1927 (2004).
27 Ricciardi, R., Auriemma, F., Gaillet, C., De Rosa, C. & Laupretre, F. Investigation of the Crystallinity of freeze/thaw poly(vinyl alcohol) hydrogels by different techniques. *Macromolecules* **37,** 9510–9516 (2004).
28 Ricciardi, R., Mangiapia, G., Lo Celso, F., Paduano, L., Triolo, R., Auriemma, F., De Rosa, C. & Laupretre, F. Structural organization of poly(vinyl alcohol) hydrogels obtained by freezing and thawing techniques: a SANS study. *Chem. Mater.* **17,** 1183 (2005).
29 O'Kane, W. J., Young, R. J., Ryan, A. J., Bras, W., Derbyshire, G. E. & Mant, G. R. Simultaneous SAXS/WAXS and d.s.c. analysis of the melting and recrystallization behaviour of quenched polypropylene. *Polymer* **35,** 1338–1352 (1994).